Ground-state binding energy of $^{4}_{\Lambda}$sH from high-resolution decay-pion spectroscopy

F. Schulz, P. Achenbach, S. Aulenbacher, J. Beričič, S. Bleser, R. Böhm, D. Bosnar, L. Correa, M.O. Distler, A. Esser, et al.

Ground-state binding energy of ${}^{4}_{\Lambda}$H from high-resolution decay-pion spectroscopy

F. Schulz[a], P. Achenbach[a,*], S. Aulenbacher[a], J. Beričič[b], S. Bleser[a,c], R. Böhm[a,1], D. Bosnar[d], L. Correa[e], M. O. Distler[a], A. Esser[a], H. Fonvieille[e], I. Friščić[d], Y. Fujii[f], M. Fujita[f], T. Gogami[f,2], H. Kanda[f], M. Kaneta[f], S. Kegel[a], Y. Kohl[a], W. Kusaka[f], A. Margaryan[g], H. Merkel[a], M. Mihovilovič[a], U. Müller[a], S. Nagao[f], S. N. Nakamura[f], J. Pochodzalla[a], A. Sanchez Lorente[a,c], B. S. Schlimme[a], M. Schoth[a], C. Sfienti[a], S. Širca[b], M. Steinen[a,c], Y. Takahashi[f], L. Tang[h], M. Thiel[a], K. Tsukada[f,3], A. Tyukin[a], A. Weber[a],

A1 Collaboration

[a] *Institut für Kernphysik, Johannes Gutenberg-Universität, 55099 Mainz, Germany*
[b] *Department of Physics, University of Ljubljana, and Jožef Stefan Institute, 1000 Ljubljana, Slovenia*
[c] *Helmholtz Institute Mainz, 55099 Mainz, Germany*
[d] *Department of Physics, University of Zagreb, 10002 Zagreb, Croatia*
[e] *LPC-Clermont, Université Blaise Pascal, CNRS/IN2P3, 63177 Aubière Cedex, France*
[f] *Department of Physics, Tohoku University, Sendai, 980-8571, Japan*
[g] *Yerevan Physics Institute, 375036 Yerevan, Armenia*
[h] *Department of Physics, Hampton University, Hampton, Virginia 23668, USA*

Abstract

A systematic study on the Λ ground state binding energy of hyperhydrogen ${}^{4}_{\Lambda}$H measured at the Mainz Microtron MAMI is presented. The energy was deduced from the spectroscopy of mono-energetic pions from the two-body decays of hyperfragments, which were produced and stopped in a ^{9}Be target. First data, taken in the year 2012 with a high resolution magnetic spectrometer, demonstrated an almost one order of magnitude higher precision than emulsion data, while being limited by systematic uncertainties. In 2014 an extended

*Corresponding author.
Email address: patrick@kph.uni-mainz.de (P. Achenbach)

[1] Present address: FAIR Facility for Antiproton and Ion Research in Europe, 64291 Darmstadt, Germany.

[2] Present address: Research Center for Nuclear Physics (RCNP), Osaka University, Osaka 567-0047, Japan.

[3] Present address: Research Center for Electron Photon Science, Tohoku University, Sendai 982-0826, Japan.

measurement campaign was performed with improved control over systematic effects, increasing the yield of hypernuclei and confirming the observation with two independent spectrometers and two targets of different thicknesses. The analysis of this data is in agreement with the previously published value for the ${}^{4}_{\Lambda}$H binding energy as well as with a consistent re-analysis of the 2012 data. When compared to the ${}^{4}_{\Lambda}$He binding energy from emulsion data, a large charge symmetry breaking effect in the $A = 4$ hypernuclear system is confirmed.

Keywords: hypernuclear mass spectroscopy, mesonic weak decay, charge symmetry breaking

1. Introduction

The structure of light Λ-hypernuclei and the precise determination of Λ hyperon binding (separation) energies has been in the focus of many recent experimental and theoretical programs [1]. Existing strongly bound *s*-shell hypernuclei include ${}^{3}_{\Lambda}$H, which is the least bound, the iso-doublet of ${}^{4}_{\Lambda}$He and ${}^{4}_{\Lambda}$H in their ground and excited states, and the iso-singlet ${}^{5}_{\Lambda}$He. The ground state in both $A = 4$ hypernuclei is a singlet, $J^{\pi} = 0^{+}$ spin system, while the first excited state is described by parallel spin orientation of the Λ hyperon and the core nucleus giving rise to a 1^{+} spin system which is excited to energies of the order of 1 MeV.

Charge symmetry of the strong interaction predicts that the Λp and Λn interaction and consequently their contribution to the binding energy of mirror hypernuclei are identical. Charge symmetry breaking (CSB) in the strong interaction occurs because of the mass difference of the fundamental up and down quarks in the hadronic and nuclear systems. In the NN interaction the CSB effect is well understood and was found to be small in the ^{3}He $-$ ^{3}H mirror pair at a level of $\Delta B^{3}_{\rm CSB} \sim 70\,$keV [2] after removal of trivial Coulomb energy contributions. In the system of $A = 4$ hypernuclei, however, old emulsion measurements found an exceptionally large difference of $\Delta B^{4}_{\Lambda} = 0.35 \pm 0.05\,$MeV between the ground state binding energies [3]. From γ-ray spectroscopy it is known, after a

very recent new determination of the transition energy in ${}^{4}_{\Lambda}$He [4], that the CSB effect has a large spin-dependence. Calculations have shown that the addition of the Λ hyperon to the ^{3}He core contracts the core slightly, leading to a decreased binding energy in ${}^{4}_{\Lambda}$He. This non-trivial Coulomb effect is in the opposite direction to the observed ground state binding energy difference [5]. Additionally, $\Lambda-\Sigma$ coupling can account for charge symmetry breaking. Since the Σ hyperon has isospin 1, while the Λ has isospin zero, the mixing of Σ states in the nuclei depends on the spin-isospin structure of the nuclear core and excited states to which the Λ may be attached.

The large value of the Λ hyperon binding energy difference and the large difference between ground and excited states of the $A = 4$ mirror pair represents one of the unresolved issues in hypernuclear physics [6, 7]. Many theoretical contemporary attempts based on a variety of hyperon-nucleon interactions were made but failed to reproduce consistently the experimental data [8–11]. Only very recently, large-scale no-core shell model calculations of ${}^{4}_{\Lambda}$He and ${}^{4}_{\Lambda}$H based on chiral nucleon-nucleon and hyperon-nucleon interactions were capable for the first time of generating sizable charge symmetry breaking in $A = 4$ hypernuclei by including charge-symmetry breaking hyperon-nucleon interactions induced by $\Lambda-\Sigma^0$ mixing [12]. This makes a confirmation of all energy levels in the $A = 4$ system with independent experimental techniques desirable, especially since there is no exact knowledge about the systematic uncertainty for the emulsion data.

2. Decay-pion measurements at MAMI

In 2012, the first high-resolution spectroscopy of pions from decays of stopped ${}^{4}_{\Lambda}$H hypernuclei was performed by the A1 Collaboration at the Mainz Microtron MAMI, Germany [13]. The MAMI beam with an energy of 1.5 GeV and an intensity of 20 μA was incident on a ^{9}Be target foil of 125 μm thickness. The process under study was a multi-step strangeness production, nuclear fragmen-

tation, and pionic weak decay reaction:

$$
\begin{aligned}
{}^{9}\mathrm{Be}(\mathrm{e},\mathrm{e}'\mathrm{K}^{+})^{9}_{\Lambda}\mathrm{Li}^{*} \quad &\rightarrow \quad \mathrm{X} + {}^{4}_{\Lambda}\mathrm{H} \\
{}^{4}_{\Lambda}\mathrm{H} \quad &\rightarrow \quad {}^{4}\mathrm{He} + \pi^{-}
\end{aligned}
$$

The foil was tilted with respect to the beam direction to minimize the energy straggling of negative pions leaving the target in direction of the spectrometers. These pions were detected alternatively in one of the two spectrometers SpekA and SpekC in coincidence with positive kaons tagged in the Kaos spectrometer. The pion spectrometers were positioned at backward angles to optimize the signal-to-background ratio for pions. The coincidence condition ensured that the observed pions originated from weak decays of hyperons and hypernuclei.

The binding energy of ${}^{4}_{\Lambda}\mathrm{H}$ was deduced from this two-body decay mode to be $B_{\Lambda} = 2.12 \pm 0.01$ (stat.) ± 0.09 (syst.) MeV with respect to the ${}^{3}\mathrm{H} + \Lambda$ mass [13]. This value is 0.08 MeV different from emulsion data, for which the most complete compilation found $B_{\Lambda} = 2.04 \pm 0.04$ MeV using only three-body decay modes [3]. A re-analysis of the data collected in 2012 was reported in Ref. [14].

In the year 2014 the experiment at MAMI was continued with improved control of systematic uncertainties, additional background suppression, and higher luminosities. Energy-loss fluctuations of pions in the scattering chamber windows have been eliminated by directly coupling the spectrometers to the chamber. Two tungsten alloy collimators were placed behind the target to reduce the background from quasi-free produced Σ^{-} decays in flight. The typical beam intensity was increased to 50 μA. In order to check systematic momentum uncertainties the acceptance of both pion spectrometers covered the ${}^{4}_{\Lambda}\mathrm{H}$ decay-momentum region simultaneously.

Fig. 1 shows the measured coincidence time distribution after identification of kaons in the Kaos spectrometer for the 2014 data set. The K^{+} and π^{-} coincidence peak is a signature for the pionic weak decay of quasifree produced hyperons and of hyperfragments. The FWHM ≈ 1.4 ns is a factor of 2 better than in the 2012 data set as a result of extensive calibrations of the time-of-flight

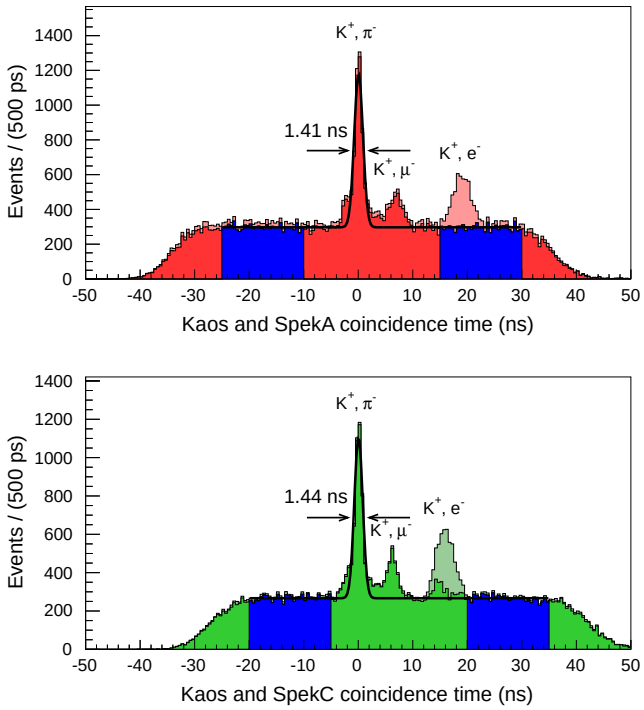

Figure 1: Coincidence time spectra between KAOS spectrometer and SpekA (top) and SpekC (bottom) after flight path corrections for K^+ and π^-. The time gates for selecting accidental coincidences are shown by the blue areas. The light shaded events consisting predominantly of the K^+ and e^- peaks were rejected by gas Čerenkov cuts. The fits to the spectra are composed of Gaussian peaks restricted to the K^+ and π^- regions on top of flat background distributions. The peaks were resolved with FWHM ≈ 1.4 ns resolution.

detectors. Details on the improvements can be found in Ref. [15].

The four panels of Fig. 2 display the pion momentum distributions in SpekA and SpekC for the two ^{9}Be targets of different thicknesses. These data consistently showed mono-energetic lines from pionic $^4_\Lambda$H decays near $p_\pi \approx 133\,\mathrm{MeV}/c$ in both spectrometers. The combined significance level for the signals is $S_\mathrm{L} = 5.1$ as determined by the profile likelihood method, confirming the observation independently from the 2012 data set. As predicted, the decay-pion peak FWHM of $\sim 80 - 90\,\mathrm{keV}/c$ in the 2014 data was also smaller then the FWHM $\sim 130 - 140\,\mathrm{keV}/c$ in the 2012 data.

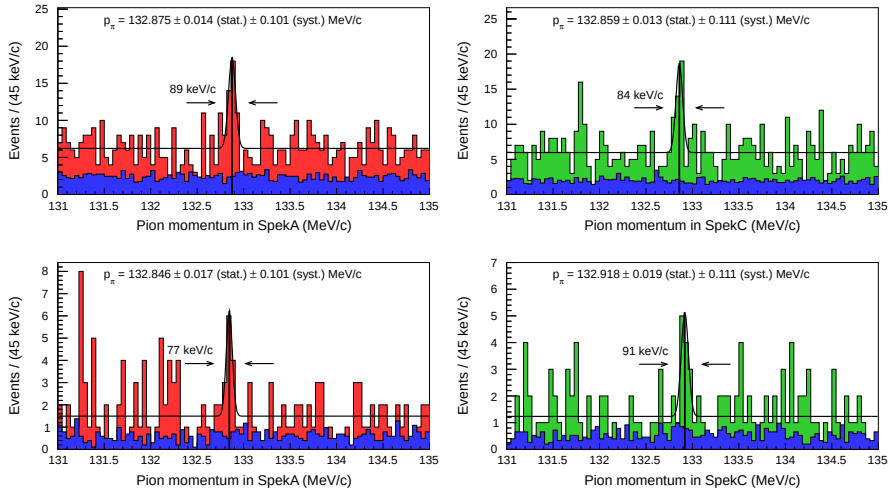

Figure 2: Pion momentum distributions in the region of interest taken with SpekA (left) and SpekC (right) using 123 μm (top) and 253 μm (bottom) thick ^{9}Be target foils from the 2014 data sets. The fits are composed of Gaussian resolution functions on top of flat background functions. The blue areas are accidental background events evaluated from the coincidence time side bands.

3. Determination of the absolute momentum scale

The absolute momentum was referenced to the momentum of electrons with energies of 195 and 210 MeV scattered off a 6 μm thick ^{181}Ta target, details are found in Ref. [15]. The typical MAMI beam energy spread was 13 keV with an energy variation of typical $\sigma_E < \pm 10$ keV that can be reduced to $\sigma_E < \pm 1$ keV using a stabilization system inside the racetrack microtron. The absolute energy of the extracted beam was known with an accuracy of $\delta E_{\mathrm{beam}} \approx \pm 160$ keV. The peaks of elastic scattered electrons had widths of order 50 keV/c (FWHM). The precision of the calibration was $\delta p_{\mathrm{calib}} \approx \pm 10$ keV/c including uncertainties in the fitting procedure and statistical errors. For SpekC the relative momentum of the elastic scattering peak was not the same as for the observed decay-pion peak, so an additional error $\delta p_{\mathrm{calib}}(\mathrm{SpekC}) \approx \pm 30$ keV/c was assigned to uncertainties in the transfer matrix. All errors were propagated to the decay-pion momentum by scaling with the absolute momentum of the peaks.

The momentum calibration of the spectrometers was consistently performed for the 2012 and 2014 data sets by scaling the momentum spectra linear with a factor determined from the analysis of the elastic scattering data. The calibration lead to a shift of the order of 1×10^{-3} when compared to the online momentum spectra.

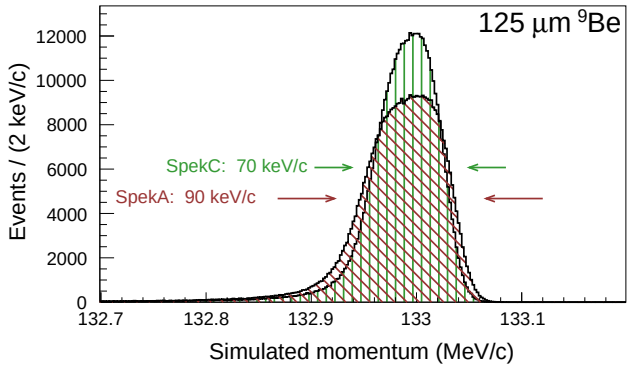

Figure 3: Simulated pion momentum distribution for a 125 μm thick ^{9}Be target and the spectrometer geometry of the 2014 data set. Due to the energy-loss and the multiple scattering of the pions inside the target the peak shape is asymmetric and the width of the peak differs for the two pion spectrometers SpekA and SpekC.

The decay of the hyperfragments was simulated with a Monte Carlo code to determine the energy-loss and the multiple scattering of the pions inside the target. The simulated pion momentum distribution for a thin target of 125 μm thickness is shown in Fig 3. A response function to closely describe the peak shape was found including a Gaussian distribution for the resolution and a Landau distribution for the energy-loss, see Ref. [15]. However, due to the low count number of observed ${}^{4}_{\Lambda}$H a simple Gaussian fit to the peak proved to be more robust to determine the most probable momentum in the data than more complex fits. The mean energy-loss was $\Delta E \sim 20\,\mathrm{keV}$ for the 125 μm thick target and $\Delta E \sim 40 - 50\,\mathrm{keV}$ for the 250 μm thick target. The systematic bias of the Gaussian mean value from the most probable momentum was $\Delta p \sim 12\,\mathrm{keV}/c$. In comparison, the energy-loss for the 2012 data set was

Table 1: Compilation of corrections added to the measured decay-pion momentum and systematic errors in the decay-pion measurement and the spectrometer calibration. The total systematic error was determined by adding the individual contributions in quadrature.

Correction or error type	SpekA	SpekC
	keV/c	keV/c
momentum-loss in 125 μm ^{9}Be	+ 36	+ 26
momentum-loss in 250 μm ^{9}Be	+ 76	+ 57
fit bias for peak from 125 μm ^{9}Be	+ 11	+ 12
fit bias for peak from 250 μm ^{9}Be	+ 11	+ 12
beam energy uncertainty in calibration	± 101	± 109
transfer matrix uncertainty	—	± 20
precision in calibration	± 6	± 7
magnetic field instability	$< \pm 5$	
uncertainty of corrections	$< \pm 5$	
total systematic uncertainty	± 101	± 111

$\Delta E \gg 100\,\mathrm{keV}$ due to the use of two vacuum window foils made of 125 μm Kapton each.

In Table 1 the corrections added to the measured decay-pion momentum and the systematic errors are tabulated. In contrast to 2012, the magnetic fields of the spectrometers were monitored continuously throughout the 2014 beam-time by NMR probes every 5 minutes. As a result, variations of the magnetic fields of the spectrometers which previously contributed 40 keV/c to the momentum error have been reduced to $\delta p_{\mathrm{stabil}} < 5\,\mathrm{keV}/c$.

4. Extraction of Λ binding energy of $^{4}_{\Lambda}$H

The binding energy B_Λ of the Λ hyperon in the ground state of $^{4}_{\Lambda}$H was deduced from the decay pion momentum p_π by

$$-B_\Lambda = \sqrt{M^2(^4\mathrm{He})\,c^4 + p_\pi^2\,c^2} + \sqrt{M_\pi^2\,c^4 + p_\pi^2\,c^2} - M(^3\mathrm{H})\,c^2 - M_\Lambda c^2$$

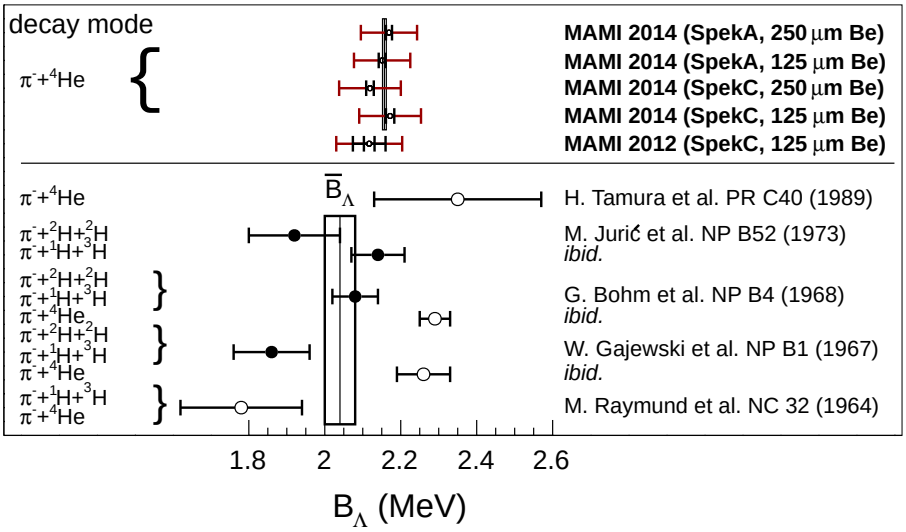

Figure 4: Λ binding energies of ${}^{4}_{\Lambda}$H from decay-pion measurements [3, 16–19]. The binding energy value from Ref. [16] was calculated from the observed momentum. Errors on the emulsion data are statistical only. The mean value as compiled by Ref. [3] excludes data from the two-body decay mode and is represented by the error band. The uncertainties on the MAMI value are statistical (inner) and total (outer), where the total error is the sum of the statistical one and the systematic one in quadrature. The MAMI 2012 data set has an additional error (middle) of $\sim 30\,\mathrm{keV}$ due to the instability of the magnetic field.

where the masses $M({}^{3}\mathrm{H}) = 2808.921\,\mathrm{MeV}/c^2$, $M({}^{4}\mathrm{He}) = 3727.379\,\mathrm{MeV}/c^2$, $M_\pi = 139.570\,\mathrm{MeV}/c^2$, and $M_\Lambda = 1115.683\,\mathrm{MeV}/c^2$ were used.

A compilation of the binding energy of ${}^{4}_{\Lambda}$H hypernuclei measured by pionic decays is presented in Fig. 4. The values measured at MAMI are compiled in Table 3. For comparison, the table lists also the luminosities for the different data sets, the number of identified pionic weak decays, and the yield of ${}^{4}_{\Lambda}$H events.

The ${}^{4}_{\Lambda}$H binding energies determined in the 2014 data set have reduced statistical and systematic uncertainties as compared to the 2012 data set. The four ${}^{4}_{\Lambda}$H binding energy values from the 2014 data sets can be combined by weigthing

with the number of observed ${}^{4}_{\Lambda}$H events:

$$\begin{aligned} B_\Lambda(\text{MAMI 2014}) &= 2.154 \pm 0.006\ (\text{stat.}) \pm 0.077\ (\text{syst.})\,\text{MeV} \quad (\text{binned fit}) \\ B_\Lambda(\text{MAMI 2014}) &= 2.157 \pm 0.005\ (\text{stat.}) \pm 0.077\ (\text{syst.})\,\text{MeV} \quad (\text{unbinned fit}). \end{aligned}$$

This binding energy is consistent with the value of

$$B_\Lambda(\text{MAMI 2012}) = 2.117 \pm 0.012\ (\text{stat.}) \pm 0.029\ (\text{stabil.}) \pm 0.081\ (\text{calib.})\,\text{MeV}$$

from the re-analysed 2012 data set. A combined momentum calibration for all five data sets was performed to minimize the systematic error in the momentum scale of the spectrometers. As a consequence the remaining systematic errors are correlated, while the uncertainty of the magnetic field instability contributing to the 2012 data set is independent from the calibration. The largest systematic error originates from the uncertainty in the MAMI beam energy affecting the absolute momentum calibration of the spectrometers by $\delta p_{\text{calib}} \sim \pm 100\,\text{keV}/c$, the sum of all other systematic errors contribute one order of magnitude less.

5. Study of systematic effects

Uncertainties in the extracted decay-pion peak position were studied by systematically varying the data cuts on kaon selection, kaon vertical angle, kaon horizontal angle, kaon minimum momentum, kaon maximum momentum, coincidence time gate, and pion vertex position. The largest effect was found when changing the kaon selection criterion, X_κ, as shown in Fig. 5. Smaller values of X_κ represent tighter cuts that reject more particles, causing a loss in ${}^{4}_{\Lambda}$H counts, whereas higher values lead to additional background. The observed variations were of the order of $\delta p_{\text{cuts}} \sim \pm 10\,\text{keV}/c$ and were almost completely covered by the evaluated fit uncertainties. Other cut conditions led to variations of $\delta p_{\text{cuts}} < \pm 5\,\text{keV}/c$. Therefore, no additional error by systematic shifts has been assumed for the combined value.

Similar studies were performed for the extracted ${}^{4}_{\Lambda}$H yield. The kaon cut conditions for each spectrometer were chosen so that the corresponding yield

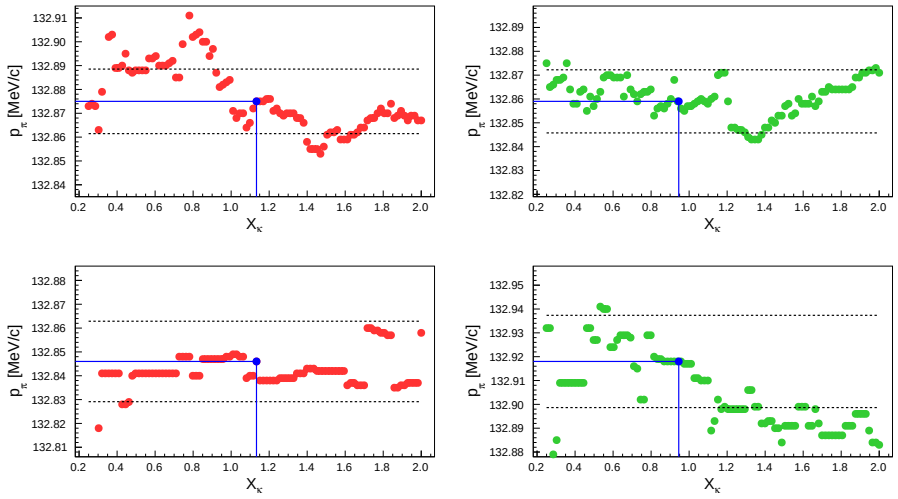

Figure 5: Extracted decay pion momentum p_π when changing the kaon selection cut X_κ. The momentum was determined by fitting the 2014 data sets for SpekA (left) and SpekC (right) with the 125 μm (top) and 250 μm (bottom) thick ^{9}Be target. Cuts used for the final decay-pion momentum determination are indicated in blue. The uncertainty of the fit for these cuts is represented by the dashed lines.

reached saturation and, therefore, had the best signal-to-background ratio. The variations in the yield of $\delta N_{\text{cuts}} \sim \pm 1$–2 events at the plateau value were well within the statistical uncertainties.

6. Conclusions

The Λ separation energy of ${}^{4}_{\Lambda}$H has been measured for the second time by high-pecision decay-pion spectroscopy at MAMI. The pions were observed in two independent spectrometers using two targets of different thicknesses, confirming the previous results in a consistent analysis of both experiments. Moreover, the results proved to be consistent after further calibration of the absolute momentum as well as in systematic studies of the used cut conditions.

When compared to the ${}^{4}_{\Lambda}$He binding energy measured with the emulsion technique and adding the information from γ-ray spectroscopy the MAMI data of ${}^{4}_{\Lambda}$H lead to the level schemes of ${}^{4}_{\Lambda}$H and ${}^{4}_{\Lambda}$He as shown in Fig. 6. While

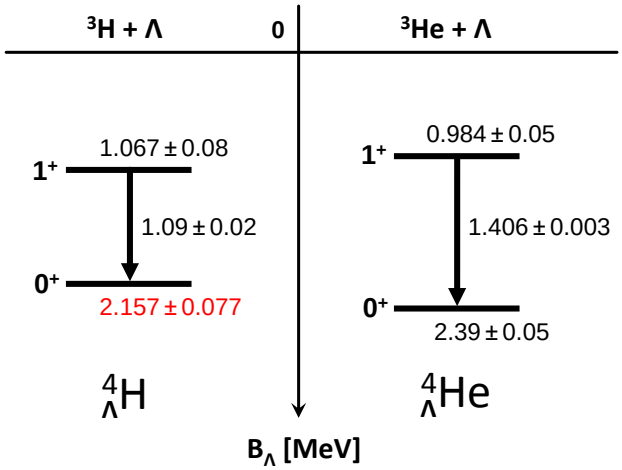

Figure 6: Level schemes of the mirror hypernuclei ${}^{4}_{\Lambda}$H and ${}^{4}_{\Lambda}$He in terms of Λ binding energy. For the ground state binding energy of ${}^{4}_{\Lambda}$H the MAMI data were used, for that of ${}^{4}_{\Lambda}$He data from past emulsion experiments [3] with a systematic error estimation of up to 40 keV [20]. The B_Λ values for the excited states were obtained from the $1^+_{\rm exc} \rightarrow 0^+_{\rm g.s.}$ γ-ray transition energies [4].

the ground state binding energy difference of $\Delta B^4_\Lambda(0^+_{\rm g.s.}) = B_\Lambda({}^{4}_{\Lambda}{\rm He}(0^+_{\rm g.s.})) - B_\Lambda({}^{4}_{\Lambda}{\rm H}(0^+_{\rm g.s.})) \approx 240\,{\rm keV}$ is smaller as measured by the emulsion technique it still supports a sizable CSB effect in the ΛN interaction. Furthermore, it suggests a negative binding energy difference between the excited states $\Delta B^4_\Lambda(1^+_{\rm exc}) = B_\Lambda({}^{4}_{\Lambda}{\rm He}(1^+_{\rm exc})) - B_\Lambda({}^{4}_{\Lambda}{\rm H}(1^+_{\rm exc})) \approx -80\,{\rm keV}$.

Most calculations performed so far resulted in much smaller binding energy differences than observed. Gazda and Gal have recently reported on *ab initio* no-core shell model calculations of the mirror pair using the charge-symmetric Bonn-Jülich leading-order chiral effective field theory hyperon-nucleon potentials plus a charge symmetry breaking $\Lambda - \Sigma^0$ mixing vertex [12]. These calculations predict a large CSB ground state splitting and a CSB splitting of opposite sign for the excited states.

During the last years the MAMI accelerator was the only place worldwide where a precise and intense continuous electron beam was available for hypernuclear physics. While the total error of the MAMI binding energy data is of the

same order than that of the compiled results from the emulsion technique, it is currently dominated by the systematic uncertainty of the absolute momentum calibration, which can be improved further. Current developments at MAMI are aiming at a higher accuracy of the calibration, which could reduce the error on the binding energy by a factor of 4.

Together with prospects for a precise measurement of the γ transition energy of ${}^{4}_{\Lambda}$H at J-PARC [21], the ${}^{4}_{\Lambda}$H level scheme could become the most accurate among hypernuclei and provide further guidance for theory and for investigating the origin of CSB in the ΛN interaction.

7. Acknowledgments

The authors would like to thank the MAMI accelerator group for their valuable contributions to the experiments. This work was supported in part by Deutsche Forschungsgemeinschaft (SFB 1044), the Carl Zeiss Foundation, European Community Research Infrastructure Integrating Activity FP7, U.S.-DOE Contract No. DEFG02-97ER41047, the Strategic Young Researchers Overseas Visits Program for Accelerating Brain Circulation (R2201), and the Core-to-Core program (21002) of JSPS.

References

[1] Proceedings of the XI International Conference on Hypernuclear and Strange Particle Physics (HYP2012) Barcelona, Spain, 1–5 October 2012, Nucl. Phys. A 914, 2013.

[2] R. Machleidt, H. Müther, Phys. Rev. C 63 (2001) 034005.

[3] M. Jurić, et al., Nucl. Phys. B 52 (1973) 1–30.

[4] T. O. Yamamoto, et al., Phys. Rev. Lett. 115 (2015) 222501.

[5] A. Bodmer, Q. Usmani, Phys. Rev. C 31 (1985) 1400–1411.

[6] A. Nogga, Nucl. Phys. A 914 (2013) 140–150.

[7] A. Gal, Phys. Lett. B 744 (2015) 352–357.

[8] E. Hiyama, M. Kamimura, T. Motoba, T. Yamada, Y. Yamamoto, Phys. Rev. C 65 (2001) 011301(R).

[9] A. Nogga, H. Kamada, W. Glöckle, Phys. Rev. Lett. 88 (2002) 172501.

[10] H. Nemura, Y. Akaishi, Y. Suzuki, Phys. Rev. Lett. 89 (2002) 142504.

[11] E. Hiyama, Y. Yamamoto, T. Motoba, M. Kamimura, Phys. Rev. C 80 (2009) 054321.

[12] D. Gazda, A. Gal (2016). arXiv:1512.01049.

[13] A. Esser, et al. (A1 Collaboration), Phys. Rev. Lett. 114 (2015) 232501.

[14] P. Achenbach, et al. (A1 Collaboration), in: Proceedings of the 12th International Conference on Hypernuclear and Strange Particle Physics (HYP2015), Sendai, Japan, 7–12 Sept. 2015, JPS Conf. Proc.

[15] P. Achenbach, et al. (A1 Collaboration), in: Proceedings of the 21st International Conference on Few-Body Problems in Physics, Chicago, Illinois, USA, 18–22 May 2015, EPJ Web Conf.

[16] H. Tamura, et al., Phys. Rev. C 40 (1989) 479–482.

[17] W. Gajewski, et al., Nucl. Phys. B 1 (1967) 105–113.

[18] G. Bohm, et al., Nucl. Phys. B 4 (1968) 511–526.

[19] M. Raymund, Nuovo Cimento 32 (1964) 555–587.

[20] D. H. Davis, Nucl. Phys. A 547 (1992) 369–378.

[21] H. Tamura, et al., Gamma-ray spectroscopy of light Λ hypernuclei II (Exp. Proposal E13-2), J-PARC, 2016.

Table 2: Two-body pionic decay momenta of ${}^{4}_{\Lambda}$H hyperfragments measured with the two spectrometers SpekA and SpekC in electron scattering off ^{9}Be targets with two different thicknesses x_{target} at the Mainz Microtron MAMI during the two beam-times in 2012 and 2014. The statistical errors were evaluated from the binned and unbinned maximum likelihood fits respectively, the systematic corrections and errors are compiled in Table 1.

			binned fit		unbinned fit			
Experiment	x_{target}	Spectrometer	p_π	δp_π(stat.)	p_π	δp_π(stat.)	δp_π(syst.)	FWHM
	μm		MeV/c	MeV/c	MeV/c	MeV/c	MeV/c	keV/c
MAMI 2012 [13]	125	SpekC	132.922	± 0.016	—	—	± 0.111 ± 0.040	143
MAMI 2012 [14]	*dto.*	*dto.*	132.923	± 0.016	132.922	± 0.019	± 0.111 ± 0.040	129
MAMI 2014	123	SpekA	132.875	± 0.014	132.875	± 0.012	± 0.101	89
MAMI 2014	*dto.*	SpekC	132.859	± 0.014	132.846	± 0.014	± 0.111	84
MAMI 2014	253	SpekA	132.846	± 0.017	132.851	± 0.011	± 0.101	77
MAMI 2014	*dto.*	SpekC	132.918	± 0.019	132.920	± 0.014	± 0.111	91

Table 3: Compilation of Λ binding energies of ${}^{4}_{\Lambda}\mathrm{H}$ evaluated from the two-body pionic decay momenta presented in Table 2 together with their statistical and systematic errors, the integrated and dead-time corrected luminosities $\int \mathcal{L}\,\mathrm{d}t$, the number of identified pionic weak decays N_{K^+,π^-}, and the hyperfragment yield $N_{{}^{4}_{\Lambda}\mathrm{H}}$. The statistical errors of the yields were evaluated from the count numbers. The combined value for MAMI 2014 was calculated by weighing with the number of observed ${}^{4}_{\Lambda}\mathrm{H}$ events.

						binned fit		unbinned fit		
Experiment	$\int \mathcal{L}\,\mathrm{d}t$	x_{target}	Spectrometer	N_{K^+,π^-}	$N_{{}^{4}_{\Lambda}\mathrm{H}}$	B_Λ	δB_Λ(stat.)	B_Λ	δB_Λ(stat.)	δB_Λ(syst.)
	fb^{-1}	μm				MeV	MeV	MeV	MeV	MeV
MAMI 2012 [13]	235	125	SpekC	—	—	2.117	± 0.012			± 0.081 ± 0.029
MAMI 2012 [14]	*dto.*	*dto.*	*dto.*	1130 ± 33	26 ± 6	2.117	± 0.012	2.117	± 0.014	± 0.081 ± 0.029
MAMI 2014	786	123	SpekA	2246 ± 257	26 ± 7	2.151	± 0.010	2.151	± 0.009	± 0.074
MAMI 2014	*dto.*	*dto.*	SpekC	3364 ± 416	25 ± 7	2.163	± 0.010	2.172	± 0.011	± 0.081
MAMI 2014	170	253	SpekA	469 ± 65	8.5 ± 4	2.172	± 0.012	2.169	± 0.008	± 0.074
MAMI 2014	*dto.*	*dto.*	SpekC	609 ± 72	8.5 ± 4	2.120	± 0.014	2.119	± 0.010	± 0.081
MAMI 2014	1912	—	—	6688 ± 810	68 ± 12	2.154	± 0.006	2.157	± 0.005	± 0.077